*toxics*

MDPI

*Review*

# Microplastics and Nanoplastics in Bone Homeostasis: Cellular Effects and Mechanistic Evidence

**Haoyu Yue [1], Wenzhuo Ju [2], Zhiyu Mu [3] and Weidong Mu [1,*]**

[1] Cheeloo College of Medicine, Shandong University, 44 West Wenhua Road, Lixia District, Jinan 250012, China
[2] Shengli Clinical College, Shandong First Medical University, 6699 Qingdao Road, Huaiyin District, Jinan 250117, China
[3] School of Biomedical Engineering, Faculty of Engineering and IT, University of Technology Sydney, Ultimo, NSW 2000, Australia
* Correspondence: cola.daughter@163.com

**Abstract**

Microplastic and nanoplastic exposures reduce osteogenic culture output and alter skeletal responses in experimental models, but they do not produce a uniform loss of bone mass. This critical narrative review searched PubMed and Europe PMC through 30 October 2026 and synthesizes 60 original journal reports spanning human detection, cell function, developmental mineralization, joint pathology, and indirect marrow or exposure evidence. Lower alkaline phosphatase or mineralization output recurs in selected cultures, sometimes alongside reduced survival; impairment per surviving cell remains unresolved. Tissue outcomes differ by compartment and disease background. Developmental co-exposure studies include both a particle-only null result with greater combined-exposure injury and cartilage findings whose direction depends on the single-exposure comparator. Chondrocyte knockdown and pharmacological experiments support selected lysosomal and inflammatory stress pathways, whereas expression-only targets provide less direct mechanistic evidence. Arthritis can persist longer without detectable exposure-related microbiome changes, so dysbiosis is not an established explanation across models. Conditioned-medium and extracellular-vesicle preparations affect recipient cells, but donor signals and transferred particles are incompletely separated. Human detection and cross-sectional associations do not establish skeletal disease causality. Priorities are function per viable cell, specific mechanistic perturbations, verified internal exposure, and functional injury outcomes. The appraised studies provide no direct functional assessment of fracture or bone-defect healing.

**Keywords:** microplastics; nanoplastics; bone homeostasis; osteotoxicity; cellular stress; osteoimmunology

Check for updates

Academic Editor: Dayong Wang

Received: 14 October 2026
Revised: 2 November 2026
Accepted: 9 November 2026
Published: 18 November 2026

**Copyright:** © 2026 by the authors. Licensee MDPI, Basel, Switzerland. This article is an open access article distributed under the terms and conditions of the Creative Commons Attribution (CC BY) license.

## 1. Introduction

Bone homeostasis depends on coordinated formation and resorption through interactions among stromal, bone-lineage, and immune cells. Research on plastic particles now examines osteogenic differentiation, skeletal development, and inflammatory remodeling alongside tissue detection. Experiments in preosteoblasts, osteocyte-like cells, and bone marrow mesenchymal stromal cells (BMSCs) document responses to particle exposure, with substantial differences in endpoints, exposure conditions, and mechanistic validation [1–4].

This review asks how far existing evidence supports disruption of bone homeostasis by microplastics (MPs) and nanoplastics (NPs). We compare measured bone-cell function and tissue outcomes with the mechanisms proposed to explain them. Human detection,

developmental mineralization, adult remodeling, and disease-associated joint changes are assessed separately because they address different biological questions.

Existing reviews describe skeletal effects and proposed inflammatory or metabolic mechanisms [5], human bone-health implications [6], and osteoimmune pathways [7]. Our contribution is to determine which experimental comparisons explain the divergent results and which proposed mechanisms are supported by functional tests. Lower osteogenic culture output is separated from impairment per viable cell, local bone loss from subchondral sclerosis, and recipient responses to transferred preparations from effects attributable to donor signals [1,3,8,9]. Two further contrasts are informative: particles can leave a developmental skeletal endpoint unchanged alone but worsen it under co-exposure, and joint inflammation can persist without a detectable exposure-related microbiome shift [10,11]. These comparisons identify limits to a single harmful-effect narrative while retaining the experimental findings that require explanation.

The comparisons also determine which experiments are most informative to repeat. Autophagy intervention studies are assessed against survival and mineralization outcomes; cartilage and synovial interventions against cell injury and local pathology; and conditioned-medium or extracellular-vesicle (EV) experiments against the material actually transferred. A tumor-derived preparation that is less suppressive than its tumor control is interpreted within that disease context, not as evidence of benefit to healthy bone [1,9,12,13]. Figure 1 summarizes the main findings and unresolved questions.

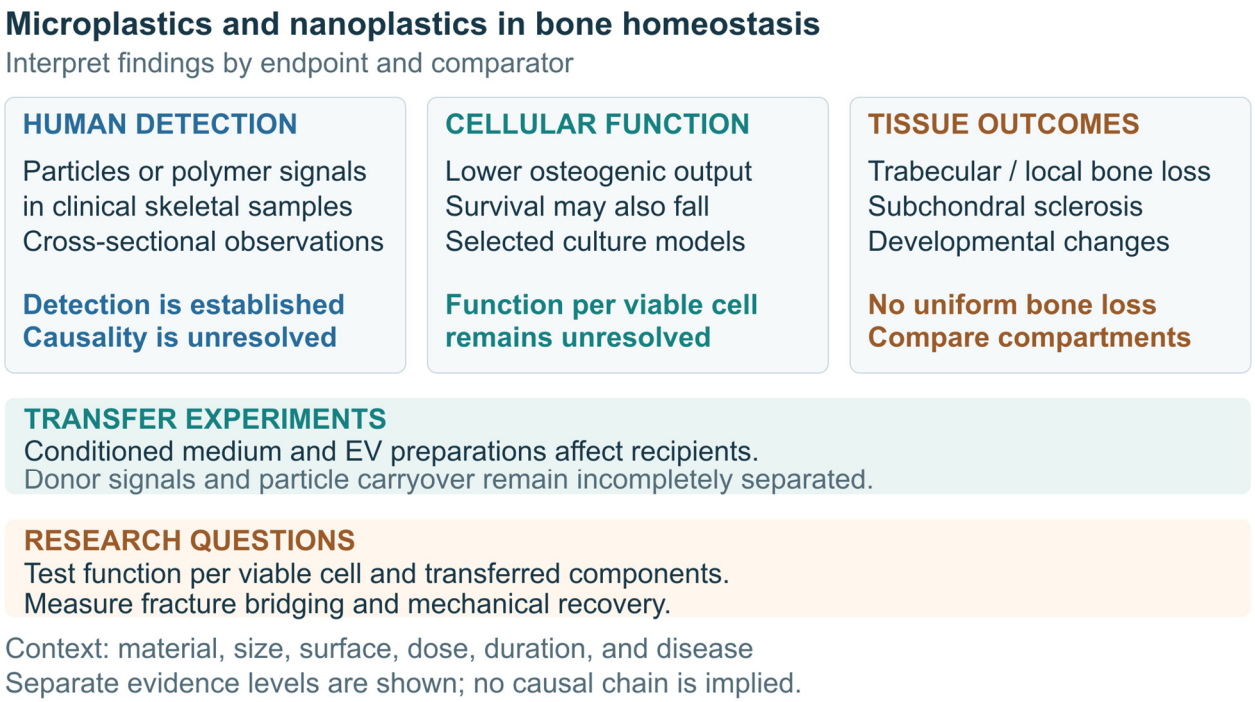



**Figure 1.** Main findings and unresolved questions about bone homeostasis. Parallel panels summarize human detection, cellular function, and tissue outcomes without implying a causal sequence between them. The transfer-experiment band describes responses to conditioned-medium or extracellular-vesicle (EV) preparations, not an established donor-signaling mechanism. The research-question band is distinct from observed outcomes. Exposure properties and disease context may affect interpretation; their independent contributions remain incompletely resolved. Figure preparation is described in Supplementary Section S4.

## 2. Literature Search and Evidence Appraisal

We searched PubMed and Europe PMC without a publication year or language restriction, using date intervals beginning on 1 January 1900. Earlier searches covered bone,

cartilage, synovial, and arthritis terms; the final sensitivity search on 30 October 2026 added vertebr*, calcif*, ossif*, mineraliz*, and mineralis* terms to the same MP and NP exposure block. Reference tracing and targeted publisher searches supplemented database retrieval. This expansion recovered an eligible 2020 vertebral-calcification study missed by the narrower endpoint vocabulary. Supplementary Sections S1–S6 provide the complete queries, fields, cutoffs, identifiers, screening decisions, and historical changes. Screening lacked independent duplication and was not preregistered.

We defined MPs as particles $\geq 1$ µm and <5 mm and NPs as particles $< 1$ µm. Classification used size information and measurement techniques reported in the methods, with nominal sizes recorded separately from measured distributions. Uncertain or overlapping distributions retained an uncertainty label. Polymer mass signals in human samples were distinguished from particle counts. Reports with MP, NP, or mixed treatment arms were interpreted by arm and counted once. Implant wear particles served as contextual comparisons for cell communication.

The synthesis includes 60 original journal reports, two associated notices, and three background reviews, yielding 65 references. The original reports have different roles: direct bone-cell or tissue outcomes, human tissue detection, adjacent cartilage or synovial outcomes, and indirect marrow or population-exposure findings. They are not 60 equivalent demonstrations of skeletal toxicity. Disc-only degeneration experiments without bone or articular-joint outcomes were excluded from the principal synthesis. Supplementary Tables S1 and S6 identify each report and its use; Table S7 records design-specific controls, and Table S9 provides selected study-level outcomes. Reports without obtainable full texts are identified separately in Supplementary Section S5 and contribute no quantitative or definitive mechanistic claims.

We grouped reports into human detection or association studies, direct bone-cell or tissue experiments, indirect marrow or immune studies, and contextual studies of implant wear particles. Extracted information included models, experimental units, particle characterization, dose and duration, controls, positive and negative findings, and mechanistic interventions. We distinguished expression and omics associations from functional phenotypes, recipient responses in transfer experiments, and pharmacological or genetic interventions. Available figures, supplements, correspondence, and corrections were checked against the reported methods and results [4,14].

This critical narrative review uses qualitative appraisal without pooling effects or assigning formal bias or certainty scores. Appraisal considers endpoint relevance, survival and assay controls, experimental units, dynamic measurements, and intervention specificity. Supplementary Table S7 records design-specific controls, Table S9 lists key outcomes and analysis sample sizes, and Table S10 defines the criteria for proposed mechanistic tests. Information missing from the available text is distinguished from a control confirmed to be absent. Supplementary Table S5 lists abbreviations and protein names.

## 3. Human Detection and Disease Associations

### *3.1. Plastic-Associated Material in Human Skeletal Samples*

Human studies identify plastic-associated material in bone marrow, skeletal tissue, synovium, blood from osteoporosis cohorts, and diseased-joint fluid [8,12,15–21]. Thermal methods measure polymer-related mass without resolving particle dimensions. Raman and infrared methods identify particles within their detectable size ranges. Table 1 distinguishes eight tissue-detection reports from a ninth, indirect population-exposure association; their results are not pooled into a prevalence estimate.

**Table 1.** Human tissue detection and exposure-association studies. Counts refer to participants unless analytical subsets are specified. The final row uses estimated dust exposure rather than skeletal-tissue measurement. Different units and detection methods are not pooled. Detailed source qualifications are retained in Supplementary Tables S2, S7, S9 and S11. OA, osteoarthritis; RA, rheumatoid arthritis; PS, polystyrene; PVC, polyvinyl chloride; PET, polyethylene terephthalate; OR, odds ratio; CI, confidence interval.

| Report and Participants | Detection or Association | Interpretation |
| --- | --- | --- |
| Guo et al. [16]; 21 patients | Thermal subset: 16/16 positive; mean 51.29 μg/g. Separate particle subset: 5 patients; mean 19.72 particles/g. | Separate subsets and units; no population disease-risk estimate. |
| Yang et al. [17]; 16 participants, 24 specimens | Bone/cartilage/disc means: 22.9/26.4/61.1 particles/g. | Multiple specimens per participant are not independent patients. |
| Li et al. [18]; 37 osteoporosis patients, 18 controls | PVC/PET mean ranks higher in patients; both $p < 0.001$. T-score correlations: −0.30/−0.26. | Ranks are not concentration ratios; no verified adjusted risk estimate. |
| Sun et al. [8]; 8 non-surgical OA samples; 2 post-arthroplasty samples separate | One non-detect among 8; positive samples: 4–66.67 particles/mL. | No healthy comparator; surgical samples kept separate. |
| Lee et al. [12]; 21 RA samples | PS-associated thermal signal in 5/21 synovial-fluid samples. | Polymer mass, not particle size or concentration per mL. |
| Zeng et al. [19]; 51 surgical patients | 8 polymer particles in 5/51 patients; a separate patient had graphite. | The six-patient particle-positive comparison is not MP-only. |
| Li et al. [20]; 21 matched-tissue donors | Bone MPs: 20/21 positive; 13.26 ± 5.49 particles/g. Thermal subset: 5 donors. | Filtered-fraction mass does not resolve NP dimensions. |
| Li et al. [21]; 45 primary arthroplasty patients | 45/45 author-classified positive; 5.24 ± 2.07 particles/g; 11–151 μm. | Includes rayon (12.0%); no healthy comparator; selected RNA-seq groups 5/5. |
| Yang et al. [22]; 14,466 older adults | Modeled PC intake: highest vs. lowest tertile arthritis OR 1.47 (95% CI 1.17–1.84). | Regional dust estimate, not skeletal detection or individual internal dose. |

Guo et al. analyzed 16 marrow samples by thermal methods and five separate samples by particle-based methods. Polymer-associated material was detected in all 16 thermal samples, with a mean of 51.29 μg/g and a range of 15.37–92.05 μg/g. The five particle-analysis samples had a separate mean of 19.72 particles/g. Yang et al. examined 24 tissue specimens from 16 participants and reported mean particle abundances of 22.9, 26.4, and 61.1 particles/g in bone, cartilage, and discs, respectively. Multiple specimens or analytical units from one participant do not increase the number of independent patients [16,17].

Detection frequencies differed across clinical settings. Sun et al. reported one non-detect among eight non-surgical osteoarthritis (OA) samples and analyzed two post-arthroplasty samples separately. Lee et al. detected a polystyrene (PS)-associated thermal signal in 5 of 21 rheumatoid arthritis (RA) samples. A Raman study of 51 patients with lumbar disc herniation identified eight polymer particles in 5 patients and graphite in another patient. Its nine-particle abundance and six-patient clinical comparison include graphite and therefore are not MP-only outcomes. Sampling selection and method-dependent recovery limit comparisons across these frequencies [8,12,19].

Li et al. studied matched blood, bone, and discs from 21 surgical donors, detecting MPs in 20/21 bone samples (13.26 ± 5.49 particles/g). Thermal analysis covered only five donors. It measured polymer mass in a nominal < 1 μm filtrate, not individual NP dimensions.

The paired design extends detection evidence but does not establish transport direction or skeletal disease causality [20].

Li et al. examined synovium from 45 patients undergoing primary hip or knee arthroplasty, without prior prostheses. All samples were positive in the authors' classification: 343 particles in total, with a mean of 5.24 ± 2.07 particles/g and sizes of 11–151 µm. The total included 12.0% rayon and should not be treated as a synthetic-polymer-only burden. Sampling and laboratory blanks were reported, but no certified size-matched recovery material was available. Higher- versus lower-burden knee-OA samples showed heat-shock-related transcriptional differences in five patients per group; this selected comparison provides exploratory association rather than a causal exposure response [21].

### *3.2. Disease Associations Require Temporality and Material Correspondence*

The osteoporosis study compared 37 patients with 18 controls. Mean ranks were higher in the osteoporosis group for polyvinyl chloride (PVC; 33.19 versus 17.33) and polyethylene terephthalate (PET; 33.36 versus 16.97), both $p < 0.001$. These values describe ranks rather than absolute concentration differences. Reported correlations with the bone mineral density (BMD) T-score were −0.30 for PVC and −0.26 for PET. The methods describe age- and sex-adjusted regression, but the checked results and available supplement contained no identifiable adjusted coefficient or confidence interval. The study documents a cross-sectional association without establishing an adjusted risk estimate or temporal sequence [18] (Supplementary Table S2).

In the OA study, eight non-surgical patients had knee effusion. Positive samples contained 4–66.67 particles/mL, with detected sizes of 20.342–175.44 µm. The two post-arthroplasty samples formed a separate comparison group; they were not healthy controls. RA thermal detection also lacked a disease-free comparator and particle-size resolution. Disease, treatment, surgery, and sampling conditions are potential determinants of the detected material. Assessment of disease associations therefore requires attention to reverse causation and differences in age, sex, occupation, smoking, renal function, and exposure to medical materials [8,12].

An indirect population study linked province-level dust measurements with data from 14,466 older adults. Estimated polycarbonate (PC) exposure in the highest versus lowest tertile was associated with arthritis after propensity-score matching and covariate adjustment (odds ratio [OR] 1.47, 95% confidence interval [CI] 1.17–1.84). The analysis used regional dust and intake assumptions, not personal particle measurements or internal skeletal dose. Arthritis subtypes were not resolved in the principal result, and other dust contaminants were analyzed separately. This extends population-association evidence without establishing a particle-specific skeletal mechanism [22].

Future human studies should define internal exposure ranges, material composition, and clinically relevant exposure timing. These measurements are needed to relate experimental exposures to those encountered in people.

## 4. Cellular Stress and Intervention Evidence

### *4.1. Recurrent Oxidative and Organelle Stress Signals*

Stress-related changes accompany altered differentiation or survival in several bone-related cell models. Young female rats exposed to approximately 1.18 µm PS at 2 mg/kg/day for 28 days developed growth-plate abnormalities alongside BiP/PERK/ATF4/CHOP-related stress indicators; only three animals were assigned per group. PET/PVC pre-osteoblast experiments and studies of 50–100 nm PS report stress responses in other bone-related cells. Differentiation and mineralization assays establish the functional consequences of these responses more directly than stress markers alone [4,18,23,24].

The measured consequences differ by cell type. Preosteoblast experiments assess induced differentiation and mineralization, osteocyte-like cells show senescence-associated and bone-regulatory changes, and OA models examine cartilage phenotype and transforming growth factor β (TGF-β) signaling. These findings describe effects on distinct cellular functions rather than successive steps in a common pathway [2,8,18].

Lipid-related findings involve distinct metabolic responses. PS-exposed osteocyte-like cells show cyclooxygenase-2 (COX2)/prostaglandin changes, while pubertal polylactic acid (PLA) exposure is associated with reduced cytochrome P450 2J5 (Cyp2j5)/epoxyeicosatrienoic acid (EET)-related indicators and osteogenic abnormalities. These findings justify further study of arachidonic acid metabolism, with separate assessment of the cell types and metabolic branches involved [2,25].

Some stress assays give contrasting results. Human bone marrow mesenchymal stromal cells (MSCs) exposed to approximately 400 nm amine-functionalized PS or its processed forms at 1.2–2.4 mg/mL for 24 h showed lower reactive oxygen species (ROS) probe signals, increased glutathione peroxidase 3 (GPX3), and an altered adipogenic fate [26]. The high concentration, surface chemistry, and possible probe interactions limit interpretation of the lower ROS signal as bone protection. Another study reported increased nitrite, DNA damage, and apoptosis without a significant superoxide change or nitric oxide (NO) blockade. The figure caption in Matovic et al. [27] labels the cells as MSC-PDL, but the methods do not specify species, donors, or tissue isolation. Interpretation of these results depends on the assay and the direction of the measured response [26,27].

Across the osteogenic experiments, lower ALP or mineralization output is the recurring functional observation. The shared result is at the culture level: survival, proliferation, cell number, and differentiation can each contribute. Static stress markers alone do not explain which contribution dominates. Thus, replication should first establish whether the output difference persists at matched viable cell numbers before assigning a selective differentiation defect [1,24,28,29].

### *4.2. Autophagy and Senescence in Relation to Cell Function*

A pubertal mouse study used 5 µm PS at 0.5 mg/animal/day for 28 days and examined related responses in preosteoblasts. Exposure to 10 µg/mL for 48 h reduced cell activity and the ALP-positive fraction or mineralized area. These results establish lower culture output under conditions that also affect survival; selective impairment of differentiation was not isolated. Baseline ALP/mineralization panels reported $n = 5$, distinct from the initial animal allocation of 12 per group [1] (Supplementary Tables S7 and S9).

Bafilomycin A1 pretreatment at 50 nM for 1 h caused LC3B/p62 accumulation in control cells, but no further increase in PS-treated cells during the 48-h challenge (protein comparisons $n = 3$). This dynamic assay extends the static marker findings, although it does not fully distinguish defects in autophagosome production, delivery, or clearance. Rapamycin pretreatment at 50 nM for 1 h improved ALP and mineralized-area outcomes ($n = 6$) alongside changes in senescence-related measures. Recovery was not independently normalized to viable osteogenic cells, and rescue was tested in cells rather than animals [1].

Osteogenic marker responses also differ by cell origin. Bottle-derived PET experiments reported different directions for some markers in bone marrow- and amnion-derived MSCs. Marker changes do not necessarily correspond to mature mineralization. The design did not isolate the contributions of size fraction, induction stage, or cell origin, or identify a specific stage of differentiation arrest [28].

The bone marrow MSC fate study reported early lipid droplets, increased peroxisome proliferator-activated receptor γ (PPARG)/CCAAT enhancer-binding protein α (CEBPA), and reduced osteocalcin (OCN) in ordinary culture. Later responses included cell death or

impaired differentiation during adipogenic induction. Osteogenic ALP and mineralization were not measured, so these findings do not establish reduced bone formation [26].

Other autophagy studies assess different endpoints. Photo-aged PS in juvenile fish was evaluated mainly through static expression and axial or skeletal-muscle outcomes, rather than bone mineralization. A PS/microcystin-LR study included bafilomycin A1 (BafA1) and tauroursodeoxycholic acid (TUDCA) comparisons, but key results appeared in external supplementary figures of the cited study [30] that were not available for this review. The main text did not establish complete rescue of co-exposure-related skeletal injury. These studies contribute to lipophagy–stress hypotheses but provide no equivalent dynamic flux evidence in osteogenic cells [30,31].

Among the osteogenic studies, the autophagy experiment combines a blockade comparison with recovery of ALP and mineralization, whereas several other studies measure markers without comparable functional recovery. This makes autophagy a useful focus for replication within osteogenic cultures, not a mechanism established across all skeletal tissues. Matched survival and an independent autophagy perturbation would determine whether the functional recovery extends beyond an increase in viable cell output [1]. Cartilage cell-death interventions address a different endpoint and are assessed separately [13].

### *4.3. Interventions as Mechanistic Tests*

Pharmacological interventions improve some exposure-related phenotypes, but their mechanistic targets differ. MLO-Y4 cells exposed to 5 μm PS at 100 μg/mL for 48 h showed senescence-related changes. Aspirin pretreatment at 20 μM for 24 h reduced the proportion of senescence-associated β-galactosidase (SA-β-gal)-positive cells by approximately 30% relative to the PS group. This result concerns cellular senescence rather than bone mass. Evaluation of autophagy and endoplasmic reticulum stress modulators likewise requires target engagement, functional outcomes, and intervention-only controls [1,2,23,24].

Two polyphenol studies using 100 nm PS reported effects in the same direction in pre-osteoblasts and juvenile-fish mineralization. The Hibiscus ALP/mineralization experiment used PS at 200 μg/mL for 2 h every 2 days, followed by medium replacement, and assessed outcomes at 14 days. The Tagetes ALP/mineralization experiment used a similar pulse schedule, with PS at 200 μg/mL in the principal protection experiment. These functional arms are comparable, although the full cell and fish protocols differ. The Hibiscus study relied mainly on autophagy markers and rapamycin comparisons, with limited dynamic flux and loss-of-function evidence. Tagetes cell experiments used the nuclear factor erythroid 2-related factor 2 (NRF2) inhibitor ML385 at 5 μM, which attenuated protection and supported an NRF2 contribution. Similar protection across the studies does not establish a shared mechanism. Supplementary Table S3 records intervention units and fish dose discrepancies [24,29].

Co-exposure to particles attenuated acute cadmium toxicity in one osteoblast study. Neonatal rat primary osteoblasts exposed to aged PS NPs at 1 mg/L and cadmium (Cd) at 0.5–1.5 mg/L for 24 h showed approximately 14.2–28.9% lower intracellular free-Cd-associated fluorescence than Cd-only cells, alongside partial attenuation of acute injury. Adsorption, aggregation, and uptake kinetics are possible explanations. Free-Cd fluorescence does not measure total elemental burden, and the study assessed neither ALP and mineralization nor long-term bone quality. The result demonstrates that co-exposure need not aggravate acute injury but provides no evidence of durable protection or repair [32].

Interventions partially restore osteogenic or survival-related outcomes through different processes. Lysosomal blockade and rapamycin test autophagy, ML385 assesses the contribution of NRF2-related protection, and aspirin targets a COX2-associated response.

In the Cd experiment, a change in available toxicant is a possible explanation for the altered effective exposure. These findings require separate mechanistic interpretation [1,2,24,32].

Intervention evidence in cartilage also varies in directness. A nominal 1 µm PS study combined 100 µg/mL, 24-h exposure with nuclear factor κB subunit 1 (NFKB1) knockdown and MD-1 treatment, whereas a 5 µm PET study mainly measured prostaglandin-endoperoxide synthase 2 (PTGS2) expression. These belong to different evidential levels even though both proposed inflammatory pathways; Section 6.3 compares their actual tests [33,34].

## 5. Context Dependence of Skeletal Outcomes

### *5.1. Developmental Effects as Evidence of Skeletal Susceptibility*

Developmental studies document disturbances in growth or mineralization, with effects varying across stages and endpoints. Young-animal PS and PLA models show changes in growth plates, endochondral ossification, and trabecular structure. Fetal skeletal staining also reveals delayed or incomplete ossification. Reduced maternal weight gain and fetal weight, together with approximately three litters per group, limit separation of general developmental delay from persistent skeletal abnormality. The findings support developmental susceptibility but do not assess adult homeostasis or recovery after injury [1,23,25,35].

Mineralization findings depend on the sampling time and skeletal element. Zebrafish exposed to nominal 50 nm PS at 5–200 µg/mL from 3 h post-fertilization (hpf) to 10 days post-fertilization (dpf) showed changes in the operculum and earlier-forming skeletal elements, while some low-dose findings for later elements were negative. Ethinylestradiol and particles were tested separately, without a combined group. A photo-aged PLA model showed no clear vertebral calcification difference at 7 dpf but fewer calcified segments later. Another PS study assessed whole-fish ALP and axial curvature, which provide less direct measures of skeletal function. These differences in endpoints and sampling times limit direct comparisons [36–38].

A zebrafish time-course study used nominal 8 µm PS at 0.2, 2, or 20 mg/L from 24 hpf. Some osteogenesis-related transcripts and swimming activity increased after 14 days of exposure. After 28 days, Sp7 and other indicators declined, and cartilage matrix abnormalities were reported. This sequence documents a changing developmental response. Because the early transcriptional and later structural endpoints measure different processes, it does not establish early protection followed by damage. The marine medaka comparison used previously published data [39].

Marine medaka exposed to approximately 7.3 µm PS at 0.2, 2, or 20 mg/L for 28 days had approximately 14% higher bone volume at the lowest dose and approximately 22% lower volume at higher doses. BMD and bone volume/tissue volume (BV/TV) did not differ significantly at any dose. Mineral/matrix changes accompanied the low-dose volume increase. The non-monotonic response is specific to bone volume and does not establish improved bone quality or a general low-dose benefit [40].

Co-exposure effects vary across developmental settings. In the 2020 zebrafish study, 65 nm PS at 2 mg/L, classified here as NP despite the original MP label, did not significantly change calcified vertebral counts alone. Exposure with butylated hydroxyanisole (BHA; 1 mg/L) from 4 hpf for 12 days reduced the count by a further 45.8% relative to BHA alone, as reported by the authors. This is a vertebral-count comparison, not a change in BMD [11]. An 80 nm PS/BDE-47 study assessed cartilage histology at 120 hpf: at 10 mg/L PS and 0.1 µg/L BDE-47 (2,2′,4,4′-tetrabromodiphenyl ether), the combined group had fewer chondrocytes than PS alone but more than BDE-47 alone. That observation was descriptive rather than a quantified cartilage-loss estimate [41]. Together, these studies

show why an adverse combined-exposure outcome cannot be interpreted without both single-exposure comparators.

Other developmental co-exposures also vary by stage. PS/tetracycline groups showed some skeletal developmental abnormalities despite negative findings for multiple PS-only endpoints. Embryonic exposure to 80 nm PS at 100 µg/mL with acetaminophen worsened some craniofacial cartilage or malformation outcomes. In a separate 7-day experiment in 21–28 dpf juveniles, co-exposure attenuated some structural abnormalities relative to acetaminophen alone. These experiments assessed toxicant-associated structural deficits rather than repair of standardized injuries. The response direction differed across stages and exposure conditions, but the comparisons did not isolate the contribution of individual factors [42–44].

### 5.2. Bone Microstructure and Mineral Composition

Chronic PS exposure connects tissue damage with changes in bone-related cells. Mice receiving 5 µm PS in drinking water at 10 mg/L for 6 months showed trabecular damage, BMSC senescence-like changes, reduced osteogenic capacity, and conditioned-medium effects on osteoclast responses. Together, these findings support disruption of the formation–resorption balance during chronic exposure. The evidence for intercellular attribution is assessed separately below [3].

Fish studies distinguish structural changes from mineralization. Continuous feeding with 20–27 µm polyethylene (PE) at 1% of the diet was associated with a 17.8% relative reduction in scale area at 90 dpf. Pronounced demineralization occurred primarily with benzo[a]pyrene-loaded particles rather than PE alone. A 21-day killifish experiment using mixed environmental particles assessed bone inorganic composition and vertebral histology. Combined Cd exposure did not consistently exacerbate outcomes. Differences in particle source, co-contaminants, and tank-level replication limit interpretation of these studies as replication of a single-polymer mechanism [45,46].

A negative osteoblast-count result illustrates the limits of histology alone. A 28-day gavage study of low-density PE (LDPE) ≤ 20 µm reported doses of 1.25–5 mg/day, without clarifying whether these were per-animal doses. Of 28 rats initially allocated, 26 remained after two deaths. Osteoblast counts did not differ significantly among groups ($p = 0.655$). Mineralization, microstructure, and mechanical properties were not measured, leaving osteogenic function untested [47].

The chronic PS experiment links trabecular structure, donor-cell function, and recipient responses within one exposure model [3]. The fish composition studies and the negative LDPE osteoblast-count study measure different functions and therefore neither replicate nor directly contradict that result [46,47]. The evidence supports model-specific remodeling changes. A claim of general bone loss would additionally require comparable structural and functional outcomes across independent exposure settings.

### 5.3. Local Resorption and Sclerosis in Pathological Settings

Periodontal bone loss and OA-associated subchondral sclerosis describe different forms of local remodeling. A 100 nm polymethyl methacrylate (PMMA) periodontal study combined immune and periodontal-cell experiments with tissue bone measurements. A joint study using 5 µm PS at 40 mg/kg/day for 16 weeks found cartilage degeneration, subchondral plate thickening, and altered porosity. Both document pathological remodeling, with different directions of change in bone quantity [8,48].

Joint studies also show that existing pathology affects the response to exposure. Yu et al. used nominal 20 nm PS at 0.5 mg/mL in drinking water. Cartilage damage and synovitis increased after destabilization of the medial meniscus (DMM), while the sham-

plus-particle group showed no significant change in cartilage score ($n = 6$ per group). The high concentration and inconsistent descriptions of exposure timing prevent a precise environmental dose–duration comparison. Lee et al. reported greater complete Freund's adjuvant (CFA)-associated ankle swelling after 5 µm PS at 50 mg/kg every other day for 40 days, as described in the figures and results (controls $n = 9$; exposed $n = 10$). A separate 60-day human-cartilage/RA-fibroblast co-implantation experiment showed greater erosion. These studies assess joint disease rather than fracture healing [12,13] (Supplementary Tables S2 and S9).

A separate collagen-induced arthritis study reported worse arthritis scores and cartilage histology during drinking-water treatment on days 1–50 (eight animals allocated per group). Conflicting dose labels and incomplete particle characterization limit exposure comparison with the Yu and Lee models. It adds an independent disease-model observation without establishing the mitochondrial explanation stated in its title [49].

A PS protein-corona study found a similar difference between healthy and diseased tissue. PS NPs at 50 mg/L in drinking water exacerbated ligature-induced periodontitis. Six-site cementoenamel junction–alveolar bone crest distances were 1.21–1.38 times those in periodontitis-only mice. The same measure did not change significantly in healthy mice. This contrast supports disease-dependent susceptibility within the model [50].

A viral-arthritis model extends the comparison to inflammatory resolution. PS-exposed mice had longer-lasting post-peak foot swelling after infection, but the peak difference was not significant and tested viral loads did not increase. The authors reported approximately 30% greater swelling area under the curve than infected controls. This measures inflammatory disease burden, not cartilage erosion, bone loss, or skeletal healing [10].

The contrast between periodontal loss and OA-associated sclerosis is biologically coherent: the studies assess different compartments and pathological remodeling processes. Greater subchondral bone quantity can coexist with cartilage injury, while periodontal loss reflects the net balance of local resorption and reconstruction. These findings challenge bone quantity as a common index of skeletal health; they do not demonstrate that a particular particle property determines the direction of the response [8,48].

Post-ligature measurements provide a recovery context, but terminal measurements without a recovery baseline cannot separate persistent resorption from reconstruction. The model provides evidence of local remodeling without directly establishing a general healing response [48].

### *5.4. Environmental Relevance of the Experimental Materials*

Differences between experimental materials and particles detected in human tissues limit environmental extrapolation. Commercial PS spheres allow controlled exposure experiments but do not reproduce the polymer mixtures, shapes, and surface histories found in human samples. Bottle-derived PET and field-collected particles expand the range of tested materials, although matched comparisons with model spheres are lacking. Implant wear particles represent a separate source. Table 2 compares sources, routes, and available exposure measurements. The reported units cannot be combined into a common dose scale, and the review derives no human-equivalent dose or safety threshold [8,17,28,46,51].

Surface modification, aging, and saliva-corona experiments show that polymer identity and nominal size alone do not adequately describe exposure. Characterization also requires surface history and the biological environment in which particles are tested. These variables do not yet predict the direction of skeletal effects. Lower intracellular free-Cd fluorescence during co-exposure is consistent with altered toxicant availability, but adsorption and uptake have not been confirmed as the explanation. Matched material comparisons are needed to separate these contributions [30,32,37,50,52].

**Table 2.** Experimental materials and exposure conditions. Nominal sizes are distinguished from measured sizes. Doses retain the source units and do not define a common human-equivalent exposure scale. Source qualifications and additional protocol details are retained in Supplementary Table S11. PS, polystyrene; PET, polyethylene terephthalate; EV, extracellular vesicle.

| Material and Study | Size Characterization | Exposure and Extrapolation Limit |
| --- | --- | --- |
| Human tissues and model PS challenge [17] | Human particles: 25.44–407.39 µm; animal PS nominal 5 µm. | Rats: intraperitoneal 500 µL of 0.13/1.3 mg/mL every 3 days for 4 weeks. Administered material differs from clinical detections. |
| Model fluorescent PS [3] | Nominal 5 µm; independent sizing not verified by this review. | Drinking water 10 mg/L for 6 months; BMSCs 30–120 µg/mL. Administered dose is not a measured skeletal burden. |
| Bottle-derived PET [28] | Reported fractions 1–2.67 µm and <1 µm; fraction definitions ambiguous. | MSC culture 10 µg/mL; main exposure 72 h. Consumer-derived material is not a field-weathered mixture. |
| PS with saliva-derived coronas [50] | TEM: 78.3 ± 6.7 nm; bare-particle DLS: 84.9 nm. | Cells 100 µg/mL, usually 24 h; drinking water 50 mg/L. Paired coronas were not independently manipulated in animals. |
| Model PS and myeloma EV preparation [9] | Nominal 50 nm; independent particle sizing absent from checked main text; supplements unverified. | Principal donor assays 100 µg/mL; transcript protocol 48 h. EV collection timings vary; free-particle co-isolation unresolved. |
| Beach-derived mixed particles [46] | Sieved <100 µm; lower bound and polymer proportions incompletely characterized. | Water 200 µg/L, with/without Cd 2 mg/L, for 21 days. Mixed materials and tank replication constrain comparison. |
| Model PS with BHA [11] | Nominal 65 nm; classified as NP; 20 µm arm not used for vertebral counts. | Water 2 mg/L PS ± 1 mg/L BHA for 12 days from 4 hpf. Particle-only null; co-exposure compared with BHA alone. |
| Model PS in viral arthritis [10] | Nominal 1 µm, internally dyed; washed and sodium-azide-free. | Drinking water 526 µg/L (~80 µg/kg/day estimated), 4 weeks before infection and continued. No detected major-organ uptake by the study assay. |

Material comparisons also require correspondence between the exposure estimate and the experimental preparation. The human synovial study identified heterogeneous particles at micrometer scales and included rayon, whereas the NFKB1 experiment used a characterized batch of approximately 1 µm PS spheres [21,33]. The PET study selected 2.4 µg/mL from a blood-mass report; that numerical match does not establish equivalent particle number, surface area, or dose in cartilage [34]. Regional dust-derived intake estimates likewise cannot be treated as measured skeletal exposure [22].

Localization measurements must correspond to the administered exposure. Separate intravenous fluorescent-particle challenges in RA studies cannot quantify delivery from their oral regimens [12,49]. Conversely, the viral-arthritis study detected no 1 µm PS in major internal organs using its fluorescence assay despite prolonged joint swelling [10]. These designs leave both local particle effects and indirect intestinal or systemic responses plausible; they do not establish that detected skeletal particles caused the observed pathology.

The examples cover human detection, model-particle exposures, consumer-derived material, and field-collected particles. Each addresses a different exposure question, and the results cannot be combined into one dose–response scale. Supplementary Tables S6 and S7 classify the evidence and document design-specific limitations.

## 6. Osteoimmune Links and Intercellular Effects

### *6.1. BMSC Conditioned Preparations and Osteoclast Responses*

BMSC-conditioned preparations increase osteoclast-precursor responses in both PS and PE experiments. In the chronic PS model, tissue and donor-cell outcomes accompany the transfer assay. Exposure to 5 µm PS at 10 mg/L in drinking water for 6 months was associated with a 25.5% relative reduction in trabecular BV/TV. Ten animals were initially allocated per group, but the sample size for the BV/TV analysis was not clearly reported. BMSCs exposed in vitro to 30–120 µg/mL PS showed reduced ALP at day 7 and mineralization at day 14. Their transferred preparations increased the tartrate-resistant acid phosphatase (TRAP)-positive area in bone marrow-derived macrophages (BMMs) cultured with added receptor activator of the nuclear factor κB ligand (RANKL) and macrophage colony-stimulating factor (M-CSF) [3].

The PE experiment used 80 nm particles, classified here as NPs. After 48 days of drinking-water exposure, animal findings consisted mainly of changes in bone transcripts. The water concentration was unclear, and structural and mechanical outcomes were not evaluated. BMSCs received 300 µg/mL for 24 h, after which RAW264.7 recipients were exposed to the conditioned medium for another 24 h. TRAP-related multinucleation and regulatory gene changes extend the transfer response to a different polymer and size, but resorption function was not measured [53].

The recurring transfer response supports further testing of stromal–osteoclast coupling. In the PS study, donor pretreatment with BAY11-7082 at 10 µM for 6 h attenuated subsequent donor RANKL expression and recipient TRAP responses, providing pharmacological support. However, added recipient RANKL, possible particle or drug carryover, and the absence of specific donor-RANKL loss-of-function experiments prevent attribution of necessity to donor RANKL. The next step is to identify which preparation component drives osteoclast differentiation and resorption [2,3,53] (Supplementary Table S7c).

### *6.2. Macrophage Effects Depend on Particle Source and Cell State*

Macrophage-associated systems show both suppression and improvement of osteogenic responses. In the periodontal study, THP-1 cells were exposed to commercial 100 nm PMMA model particles at 100–200 µg/mL for 48 h before conditioned-medium transfer to human periodontal ligament cells (hPDLCs). Recipient osteogenic markers changed, and ALP/mineralization findings were reported. Marker-assay timing differed between the results and methods (24 versus 48 h), and the full transfer-induction protocol was not established. Implant PE wear-particle co-culture, in contrast, improved MSC osteogenesis, particularly under alternatively activated macrophage (M2)-related conditions and a lipopolysaccharide (LPS) background [48,51] (Supplementary Table S2).

The periodontal transfer experiment and the implant co-culture study produce different osteogenic responses, but the contrast changes material, donor stimulation, recipient origin, and culture configuration simultaneously. It therefore cannot identify macrophage polarization as the cause. The useful common question is whether a recipient response persists when the exposure material, viable donor output, and recipient population are matched [48,51].

Periodontal tissue findings support the relevance of the PMMA model, but toxicity and carryover complicate the transfer assay. The supplement reports clarification at 1000 rpm for

5 min, which does not establish removal of 100 nm particles. The 200 μg/mL exposure also approaches the reported half-maximal viability-inhibiting concentrations of approximately 203–213 μg/mL in hPDLCs and THP-1 cells. Quantification of viable donor output and transferred particles is needed before attributing recipient effects to a specific immune mediator [48] (Supplementary Table S7c).

The surrounding disease environment alters particle behavior in saliva-corona experiments. PS at 100 μg/mL was incubated with healthy or periodontitis-associated saliva before 24-h macrophage exposure. Disease-associated coronas increased uptake and inflammatory responses; pharmacological uptake inhibition added evidence about this process. Paired corona conditions were not directly manipulated in the drinking-water animal experiment. Nor did corona depletion/reconstitution or receptor blockade link complement enrichment, classically activated macrophage (M1) markers, TRAP, and bone loss. The study establishes microenvironment-dependent responses without resolving macrophage–osteoclast communication [50].

### *6.3. Inflammatory Signaling in Joint and Immune Models*

General immunotoxicology studies report material-dependent inflammatory responses. A multi-material THP-1 screen using NOD-like receptor family pyrin domain-containing 3 (NLRP3) knockout at 50 μg/cm$^2$ for 24 h found NLRP3-dependent responses to particular amine-modified PS particles, with no comparable response to most other particles. A primary-cell study of 100 nm PS found suppression of both M1 and M2 macrophage responses under induction conditions. Neither study measured bone function [52,54].

The general immune studies and local periodontal studies use different materials and stimulation conditions. Across these settings, M1/M2 macrophage-phenotype labels cannot substitute for measurement of recipient skeletal function. Surface-dependent activation is a possible contributor, but its independent role in bone outcomes has not been isolated [48,52,54].

Interventions in the OA study support specific signaling steps. Interleukin-1β (IL-1β) neutralization reversed some expression responses, secreted phosphoprotein 1 (SPP1) knockdown reduced STAT3 phosphorylation, and TGF-β-related interventions altered downstream readouts. These perturbations provide stronger mechanistic evidence than transcript associations alone. Transfer from chondrocytes to BMSCs was not tested [8].

The cartilage study tested lysosomal and downstream cell-death processes. Cathepsin B (CTSB) small interfering RNA (siRNA; 50 nM, scrambled control) reduced death in exposed chondrocytes and NLRP3- and gasdermin D (GSDMD)-related changes, while restoring aggrecan and collagen II expression (key comparisons $n = 3$). Dimethyl fumarate reduced downstream injury without reversing cathepsin redistribution, supporting an upstream lysosomal contribution. Quercetin improved survival-related outcomes and DMM cartilage pathology. Its pleiotropic effects and the absence of an in vivo CTSB-specific intervention limit attribution of tissue protection to this pathway. Matrix recovery was not separated from survival recovery [13].

The NFKB1 study provides a second targeted chondrocyte approach. Primary rat chondrocytes exposed to approximately 1 μm PS at 100 μg/mL for 24 h showed reduced viability, ER-stress responses, apoptosis, and altered matrix-gene expression. The main methods and results describe 50 nM NFKB1 siRNA for 48 h before challenge and attenuation of stress markers and inflammatory secretion; Supplementary Figure S7 of Pan et al. [33] was not independently available. MD-1 treatment reduced apoptosis and partly reversed matrix-gene changes, but donor independence, complete drug conditions, and recovery per viable cell remain unresolved. The study included no in vivo OA exposure model [33].

Perinatal findings differ by dose and endpoint. Maternal gestational/lactational exposure to nominal 100 nm PS at 10 or 100 mg/L in drinking water increased offspring BMD and BV/TV at the lower dose on postnatal day 21 (P21). The higher dose reduced growth-plate thickness, while TRAP-positive osteoclast counts did not change significantly. Reduced neutrophil extracellular trap (NET)-related expression or omics signals remain associations. Attribution to NET-mediated bone injury requires extracellular NET quantification, specific intervention, or neutrophil–bone-cell transfer experiments [55].

In RA fibroblasts, MTT activity did not decline significantly across the tested 10–1000 μg/mL range at 48 h. Five-micrometer PS increased cytokine secretion and migration/invasion, while 50 μm particles had little effect on the reported cytokine outputs. BAY11-7082 and SB203580 attenuated cytokine secretion, supporting inflammatory-pathway involvement in this model [12]. The 2023 RA study similarly found increased FLS proliferation, invasion, and inflammatory output at 0.5 mg/mL for 48 h, with worsened arthritis and cartilage histology in mice. However, no identifiable mitochondrial functional measurement or targeted mitochondrial perturbation was described in the available main PDF, despite the mitochondrial wording in its title [49]. These reports support activated synovial responses more clearly than a shared mitochondrial mechanism. The MRL/lpr synovitis and separate PET/LPS chondrocyte studies remain mainly expression-associated evidence [56,57].

PET experiments add a marker-level contrast. Commercial approximately 5 μm PET at 2.4 μg/mL increased PTGS2-related readouts in human chondrocyte and synovial cell lines. Figure 8 of Di et al. [34] includes PET-only and combined disease-stimulation groups, but its IL-1β description is not fully specified in the main exposure protocol. The main PDF describes neither PTGS2 loss of function nor a cartilage or bone functional rescue. These data support an exposure-associated expression response; molecular docking of a PET representation does not establish particle binding to PTGS2 or PTGS2-dependent arthritis [34].

### *6.4. Pathological EV Preparations and Recipient Responses*

In a multiple-myeloma model, preparations from NP-exposed donors caused less osteogenic suppression than preparations from control tumor donors. Human OPM2 cells were exposed to nominal 50 nm PS. Principal donor-cell assays used 100 μg/mL, but the 48-h transcript protocol did not define every EV-collection arm. The authors report transferring equal extracellular vesicle (EV) numbers to mouse preosteoblasts. After 24-h recipient education, control tumor preparations reduced Runt-related transcription factor 2 (Runx2) mRNA by approximately 25% relative to recipients without EVs. Preparations from NP-exposed donors were less suppressive. A separate 7-day induction assay showed higher mineralization with NP-donor preparations than with control tumor preparations. A 30 nM microRNA-505 (miR-505) mimic partly restored suppression under a separate 48-h EV-treatment protocol [9] (Supplementary Table S2).

This result concerns reduced inhibition by a tumor preparation and is therefore compatible with injury from direct particle exposure in healthy osteogenic cells. Equal EV numbers control for differences in the administered vesicle count, while the recipient mimic experiment supports further testing of cargo function. Free particles and co-isolated components were not fully separated, and recipient mimic treatment does not establish the necessity of endogenous donor cargo. Follow-up experiments should separate these fractions and manipulate donor cargo directly [9] (Supplementary Table S7c).

## 7. Indirect Evidence from the Bone Marrow Microenvironment

### *7.1. Hematopoietic and Genotoxic Endpoints*

Marrow studies report selective hematopoietic changes. Mice given 5 μm PS at 0.1 or 0.5 mg/animal/day for 28 days showed reductions in some colony types at the higher dose, with negative findings at the lower dose and for other colonies. A 42-day study of 5/10 μm and 80 nm PS at 60 μg/animal/day reported selected colony and population changes. Colony formation measures function; relative cell frequencies cannot replace absolute counts or stromal osteogenic assays [58,59].

Comet assays and hematopoietic stem/progenitor cell (HSPC) studies document marrow responses without assessing bone formation. After single-dose gavage at 10, 100, or 1000 mg/kg and 24 h observation, comet findings were not significant in MP-only groups, while some NP and mixed groups showed greater DNA injury. A separate 80 nm PS study found dose-dependent changes in blood and HSPC populations without transplantation or clonal-function testing. These distinct marrow effects do not establish a shared hematopoietic mechanism of skeletal dysfunction [60,61].

An additional rat study used commercial PS NPs (reported TEM size 20 nm; hydrodynamic size 50 nm) at 10, 20 or 30 mg/kg per gavage, three times weekly for 90 days. Five animals per group were sampled at days 30, 60 and 90. Descriptive femoral marrow histology showed prominent megakaryocytes and fewer adipocytes at later sampling, alongside higher serum inflammatory markers and lower immunoglobulin G (IgG). This extends marrow observations beyond cytopenia; adipocyte depletion does not establish increased stromal osteogenesis or altered bone turnover [62].

### *7.2. Gut to Marrow Signaling and Skeletal Inference*

Gut-related studies differ in causal testing. Co-exposure skeletal-development and multi-size hematopoietic studies mainly report parallel microbiota, metabolic, and inflammatory changes. A hematopoietic stem cell (HSC) study using approximately 500 nm PS included microbiota transfer, transplantation assays, and metabolite interventions. Gavage delivered 0.01 or 0.1 mg in 100 μL per animal per administration on alternate days for 5 weeks. Direct culture and different administration routes did not reproduce the same effects, strengthening the evidence for an indirect intestinal pathway [42,59,63].

A melatonin/mixed-probiotic study used nominal 80 nm PS at 60 μg/animal/day for 42 days. Concurrent treatment improved selected HSPC frequencies and microbiota/metabolite changes, but multipotent progenitor (MPP) frequencies did not clearly recover. Without microbiota transfer, depletion, or single-metabolite testing, network-derived intermediates remain unvalidated. Concurrent systemic treatment provides less specific mechanistic evidence than transplantation and microbiota manipulation [64].

Microbiota transfer and transplantation provide more specific evidence for an intestinal contribution to HSC function than parallel microbiota changes or concurrent treatment [63,64]. Joint inflammation, however, need not follow the same pathway. In the viral-arthritis model, 1 μm PS at 526 μg/L in drinking water, estimated at approximately 80 μg/kg/day, was given for four weeks before chikungunya infection and continued afterward. Foot swelling persisted longer without significantly greater tested viral burdens or a detectable MP-related microbiome shift. This supports a disease-course effect while leaving its intestinal or systemic mediator unresolved [10]. HSC dysfunction, dysbiosis, and joint inflammation should therefore be tested as distinct outcomes rather than successive steps in an assumed gut–bone pathway.

## 8. Integrated Assessment of Evidence for Bone Homeostasis

### *8.1. Findings Supported by Functional Evidence*

The functional evidence supports three conclusions at different levels. First, reduced ALP or mineralization output recurs in selected osteogenic cultures, although survival contributes in some experiments [1,24,29]. Second, tissue responses include trabecular deterioration, periodontal loss, and subchondral sclerosis in different compartments [3,8,48]. Third, targeted cartilage interventions support selected stress responses, whereas the PTGS2 expression study and the incompletely characterized RA model do not establish their proposed mediators [13,33,34,49]. Thus, recurrent phenotypes and mechanistic verification need separate judgments.

Divergent findings are interpretable when the comparator and endpoint are retained. A particle-only null result coexists with greater BHA-associated vertebral impairment, while BDE-47 co-exposure yields different cartilage comparisons against the two single exposures [11,41]. Reduced suppression by tumor-derived EV preparations is relative to control tumor preparations, not a benefit to healthy bone [9]. Early transcripts and later cartilage abnormalities are different endpoints sampled at different times [39]. These distinctions explain why the findings need not conflict, without independently assigning the difference to polymer, size, or developmental stage. Table 3 summarizes the resulting judgments.

**Table 3.** Functional findings and the comparisons needed to resolve their interpretation. Conclusions are qualitative, not formal certainty ratings. Proposed tests are not controls already completed by the source studies. Supplementary Tables S9–S11 retain study-level details.

| Evidence Domain | Supported Finding | Interpretation and Next Discriminating Test |
| --- | --- | --- |
| Osteogenic cultures [1,24,29] | Lower ALP/mineralization output; interventions improve some outcomes. | Survival contributes in some conditions. Test output at matched viable cell numbers. |
| Local remodeling [3,8,12,13,48] | Trabecular/periodontal loss and OA-associated sclerosis occur in distinct models. | Compartments differ. Compare structural outcomes within matched disease and exposure settings. |
| Development and co-exposure [11,36,39–41] | Particle-only null results and comparator-dependent cartilage changes accompany other developmental abnormalities. | Keep skeletal element, exposure duration and both single-exposure comparators; test proposed mediators separately. |
| BMSC transfer [3,53] | Recipient TRAP responses recur; one study includes donor inhibitor treatment. | Added RANKL and carryover complicate attribution. Test purified preparations, donor mediator loss of function, and resorption. |
| Macrophage-associated systems [48,51] | Periodontal transfer and implant co-culture differ in osteogenic response. | Material, stimulation, and recipients also differ. Polarization alone cannot explain the contrast. |
| Myeloma EV preparations [9] | Equal-count NP-donor preparations are less suppressive than control tumor preparations. | This is not a general particle benefit. Separate EVs, free particles, and non-EV material before testing donor cargo. |
| Chondrocyte mechanisms [13,33,34] | Targeted CTSB/NFKB1 experiments provide more direct tests than PTGS2 expression. | Verify the reported knockdown supplement, replicate independently, and separate matrix recovery from survival. |
| Intestinal and joint responses [10,63] | HSC function and viral-arthritis persistence have different functional evidence. | A microbiome shift was not detected in the viral model; test each intestinal mediator against its own recipient outcome. |

### *8.2. Mechanistic Tests and Selection Criteria*

Mechanistic follow-up should be selected within each endpoint domain using relevant functional outcomes, dynamic or perturbational measurements, target-specific or orthogonal interventions, and independent biological or model replication. These criteria are not

combined into a score. BMSC–osteoclast transfer warrants preparation purification and mediator testing because recipient responses recur in PS and PE experiments and one study includes a donor intervention. Recipient resorption is the next functional endpoint beyond TRAP area [3,53] (Supplementary Table S10).

Different endpoint domains favor different follow-up experiments. In osteogenic cultures, the autophagy study combines a dynamic blockade comparison with ALP/mineralization recovery that was not normalized independently of survival [1]. In chondrocytes, CTSB knockdown connects a targeted perturbation with cell-death and matrix readouts [13]. The newly appraised NFKB1 study adds a reported genetic perturbation alongside pharmacological protection, although the underlying knockdown supplement remains unverified and no animal exposure model was tested [33]. In RA fibroblasts, pathway inhibitors support a secretion response [12]. These designs provide more direct endpoint evidence than PTGS2 expression or network predictions alone [34,56,57]. Priorities are domain-specific: independent replication and survival-matched functional measurements remain preferable to adding further pathway markers.

Pathological EV preparations require follow-up within their disease context. Equal-count comparisons and recipient mimic experiments justify testing donor cargo after separating EV-enriched, EV-depleted, and free-particle fractions. Matching viable donor output would also assess secretion quantity. Supplementary Tables S4, S8 and S10 specify tests that distinguish preparation effects, contributions of donor-derived signals, and the necessity of individual mediators [9].

### *8.3. Shared Limitations and Environmental Interpretation*

Cell viability, assay interference, experimental-unit independence, and residual transferred material limit mechanistic attribution across studies. Donor signals, EV-associated material, direct cell injury, and systemic pathways are not mutually exclusive; mediator blockade tests a specific contribution. Information missing from a report is distinguished from a control confirmed to be absent. Supplementary Tables S2 and S7 document numerical ambiguities and design-specific limitations.

Controlled exposures establish biological responses in experimental models, but do not quantify human skeletal risk. Internal-dose measurements and matched-material comparisons remain major gaps. Expanded endpoint searches and full-text reassessment broadened the temporal and joint coverage, including the 2020 vertebral study and additional human synovial and disease-model reports. The review remains limited by targeted supplementation, screening without independent duplication, unavailable full texts identified in Supplementary Section S5, and incomplete access to external supplements. The 60 reports have not all undergone a new independent risk-of-bias or certainty assessment (Supplementary Sections S1–S6).

### *8.4. Bone Repair as a Separate Research Question*

The appraised studies provide no direct functional assessment of fracture or bone-defect healing. Injury studies should measure bridging and mechanical recovery while distinguishing pre-existing bone quality from new tissue formation. These experiments can proceed alongside mechanistic work to determine whether exposure improves or impairs recovery. Attribution to cell communication requires controls for carryover and viable donor output, while direct cell death remains another potential contributor (Supplementary Tables S4 and S8).

## 9. Conclusions

Experimental evidence supports lower osteogenic culture output and altered skeletal responses under selected exposures. It does not establish a selective loss of osteogenic capacity per viable cell or a uniform decline in bone mass. Developmental co-exposure outcomes depend on the endpoint and comparator, while trabecular deterioration, periodontal loss, subchondral sclerosis, and prolonged joint inflammation describe different biological processes. Retaining particle-only null results and comparator-dependent effects makes this context dependence explicit.

Mechanistic evidence is most informative when perturbation changes a relevant function: examples include chondrocyte injury, inflammatory secretion, and osteogenic culture recovery. Expression-only findings, transfer-preparation effects, and parallel microbiome changes warrant different interpretations. Human tissue detection and cross-sectional associations do not establish disease causality. Follow-up should prioritize independent replication, viable-cell normalization, specific mediator tests, and exposure verification. Direct functional assessment of fracture or bone-defect healing remains absent from the appraised studies.

**Supplementary Materials:** The following supporting information can be downloaded at: https://www.mdpi.com/article/10.3390/toxics14111016/s1, Section S1: Search documentation; Section S2: Eligibility and interpretation; Section S3: Full text availability and appraisal limits; Section S4: AI assistance and figure preparation; Section S5: Record matching screening and targeted supplementation; Section S6: Final endpoint expansion and historical coverage; Table S1: Source and manuscript crosswalk; Table S2: Numerical interpretation and unresolved units; Table S3: Polyphenol protocols by endpoint; Table S4: Basis for the proposed comparisons in Table S8; Table S5: Abbreviations corresponding to the main text; Table S6: Evidence use and report provenance; Table S7 (S7a–S7c): Design-specific controls and reporting limitations; Table S7a: Human sampling and analysis; Table S7b: Animal allocation and analysis; Table S7c: Cell and ex vivo controls; Table S8: Proposed controls and bone repair research comparisons; Table S9: Selected study level outcome matrix; Table S10: Criteria for proposed mechanistic comparisons; Table S11: Extended details underlying compact main tables. References cited in the Supplementary Materials use the same numbering as the main reference list [1–64].

**Author Contributions:** Conceptualization, W.M.; investigation, H.Y.; writing—original draft preparation, H.Y.; writing—review and editing, W.J., Z.M., and W.M.; visualization, H.Y.; supervision, W.M. All authors have read and agreed to the published version of the manuscript.

**Funding:** This research received no external funding.

**Institutional Review Board Statement:** Not applicable.

**Informed Consent Statement:** Not applicable.

**Data Availability Statement:** No new data were created or analyzed in this study. The literature search records and evidence extraction materials are provided in the Supplementary Materials.

**Acknowledgments:** OpenAI Codex (OpenAI; San Francisco, CA, USA) was used to assist with English translation, language editing, organization of literature evidence records, and code for the explanatory figure. The figure was constructed using editable vector elements and does not contain generated primary research images or experimental measurements. The authors are responsible for the accuracy and integrity of the final manuscript.

**Conflicts of Interest:** The authors declare no conflict of interest.

## References


1. Pan, C.; Wu, Y.; Hu, S.; Li, K.; Liu, X.; Shi, Y.; Lin, W.; Wang, X.; Shi, Y.; Xu, Z.; et al. Polystyrene microplastics arrest skeletal growth in puberty through accelerating osteoblast senescence. *Environ. Pollut.* **2023**, *322*, 121217. [CrossRef] [PubMed]
2. Li, L.; Su, Y.; Huang, J.; Xu, W. Polystyrene microplastics induces senescence of osteocytes by activating the cyclooxygenase-2 signaling pathway. *Ecotoxicol. Environ. Saf.* **2025**, *300*, 118466. [CrossRef] [PubMed]
3. Pan, C.; Hong, R.; Wang, K.; Shi, Y.; Fan, Z.; Liu, T.; Chen, H. Chronic exposure to polystyrene microplastics triggers osteoporosis by breaking the balance of osteoblast and osteoclast differentiation. *Toxicology* **2025**, *510*, 154017. [CrossRef] [PubMed]
4. Giannandrea, D.; Parolini, M.; Citro, V.; De Felice, B.; Pezzotta, A.; Abazari, N.; Platonova, N.; Sugni, M.; Chiu, M.; Villa, A.; et al. Nanoplastic impact on bone microenvironment: A snapshot from murine bone cells. *J. Hazard. Mater.* **2024**, *462*, 132717. Corrigendum in *J. Hazard. Mater.* **2024**, *480*, 135906. https://doi.org/10.1016/j.jhazmat.2024.135906. [CrossRef] [PubMed]
5. Zhao, H.; Mu, S.; Wang, W.; Li, X. Potential threats of environmental microplastics to the skeletal system: Current insights and future directions. *Front. Endocrinol.* **2025**, *16*, 1658056. [CrossRef] [PubMed]
6. Gogakos, A.I.; Polyzos, S.A.; Anastasilakis, D.A.; Anastasilakis, A.D. Exploring the relationship between microplastic exposure and bone health. *Endocr. Connect.* **2026**, *15*, e260187. [CrossRef] [PubMed]
7. Fan, J.; Li, J.; Hao, C.; Hui, Y. Osteoimmunological impacts of micro/nanoplastics: Systemic translocation, inflammatory responses, and bone remodeling disruption. *Front. Immunol.* **2026**, *17*, 1862512. [CrossRef] [PubMed]
8. Sun, K.; Zhou, S.; Yang, M.; Li, Y.; Yu, X.; Zhao, K.; Shen, M.; Li, K.; Fu, K.; Zhan, J.; et al. Microplastics induce osteoarthritis by modulating chondrocyte inflammation and disrupting TGF-β signaling in mesenchymal stem cells. *J. Adv. Res.* 2026, *online ahead of print*. [CrossRef] [PubMed]
9. Villa, A.; Citro, V.; Sauro, G.; Ciana, P.; Chiaramonte, R.; Giannandrea, D.; Platonova, N.; Lesma, E.; Bernardelli, C.; De Felice, B.; et al. Nanoplastics perturb extracellular vesicle-mediated communication in the in vitro and ex vivo bone marrow microenvironment of multiple myeloma. *J. Hazard. Mater.* **2026**, *514*, 142667. [CrossRef] [PubMed]
10. Rawle, D.J.; Dumenil, T.; Tang, B.; Bishop, C.R.; Yan, K.; Le, T.T.; Suhrbier, A. Microplastic consumption induces inflammatory signatures in the colon and prolongs a viral arthritis. *Sci. Total Environ.* **2022**, *809*, 152212. [CrossRef] [PubMed]
11. Zhao, H.-J.; Xu, J.-K.; Yan, Z.-H.; Ren, H.-Q.; Zhang, Y. Microplastics enhance the developmental toxicity of synthetic phenolic antioxidants by disturbing the thyroid function and metabolism in developing zebrafish. *Environ. Int.* **2020**, *140*, 105750. [CrossRef] [PubMed]
12. Lee, S.H.; Jeong, G.H.; Nam, M.K.; Kwak, M.H.; Kim, C.; Park, S.H.; Yeo, J.; Choi, S.; Jung, H.S.; Rhim, H.; et al. Polystyrene microplastics activate NF-κB/MAPK signaling in synovial fibroblasts, promoting inflammation and joint destruction in rheumatoid arthritis. *J. Hazard. Mater.* **2025**, *499*, 140194. [CrossRef] [PubMed]
13. Yu, T.; Zhang, H.; Sun, W.; Xie, J.; Yu, Y.; Xu, J.; Zhou, Y.; Zhang, X. Nanoplastics exposure accelerates the progression of osteoarthritis via lysosomal destabilization-mediated pyroptosis. *J. Adv. Res.* 2026, *online ahead of print*. [CrossRef] [PubMed]
14. Kiliç, H. Concerns about the methodology used in the paper "Discovery and analysis of microplastics in human bone marrow" (J Hazard Mater 2024). *J. Hazard. Mater.* **2026**, *502*, 140916. [CrossRef] [PubMed]
15. Lu, S.; Wei, Y.; Xu, R.; Li, M.; Qv, Y.; Zha, Y.; Gong, M.; Wang, N.; Lu, X.; Jiang, X.; et al. New insights: Discovery of microplastics in human bone and skeletal muscle. *Innov. Med.* **2024**, *2*, 100100. [CrossRef]
16. Guo, X.; Wang, L.; Wang, X.; Li, D.; Wang, H.; Xu, H.; Liu, Y.; Kang, R.; Chen, Q.; Zheng, L.; et al. Discovery and analysis of microplastics in human bone marrow. *J. Hazard. Mater.* **2024**, *477*, 135266. [CrossRef] [PubMed]
17. Yang, Q.; Peng, Y.; Wu, X.; Cao, X.; Zhang, P.; Liang, Z.; Zhang, J.; Zhang, Y.; Gao, P.; Fu, Y.; et al. Microplastics in human skeletal tissues: Presence, distribution and health implications. *Environ. Int.* **2025**, *196*, 109316. [CrossRef] [PubMed]
18. Li, Y.; Piao, G.; Hu, F.; Chen, W.; Wang, Q.; Zhang, X.; Ling, H.; Liang, J. The silent invasion of microplastics polyvinyl chloride and polyethylene terephthalate: Potential impact on osteoporosis. *J. Hazard. Mater.* **2025**, *492*, 138074. [CrossRef] [PubMed]
19. Zeng, Z.; Huang, R.; Song, C.; Xiang, X.; Li, Z.; Wang, Y.; Wang, Y.; Zhu, L.; Wang, X.; Li, X.; et al. Microplastics in nucleus pulposus tissue of humans revealed by Raman mosaic imaging screening. *Sci. Rep.* **2026**, *16*, 27441. [CrossRef] [PubMed]
20. Li, X.; Wang, Y.; Feng, Z.; Zhang, J.; Xing, B.; Ding, T. Microplastics and nanoplastics in matched human blood, bone, and intervertebral discs: Accumulation patterns and risks. *npj Emerg. Contam.* **2026**, *2*, 22. [CrossRef]
21. Li, Z.; Zheng, Y.; Maimaiti, Z.; Fu, J.; Yang, F.; Li, Z.-Y.; Shi, Y.; Hao, L.-B.; Chen, J.-Y.; Xu, C. Identification and analysis of microplastics in human lower limb joints. *J. Hazard. Mater.* **2024**, *461*, 132640. [CrossRef] [PubMed]
22. Yang, L.; Wang, Y.; He, L.; Xiang, L.; Wang, L.; Yao, Y.; Sun, H.; Zhang, T. Dust-borne emerging contaminants: An underrecognized risk factor for non-communicable diseases in older Chinese adults. *Environ. Sci. Process. Impacts* **2025**, *27*, 3083–3094. [CrossRef] [PubMed]
23. Zhang, Q.; Lang, Y.; Tang, X.; Cheng, W.; Cheng, Z.; Rizwan, M.; Xie, L.; Liu, Y.; Xu, H.; Liu, Y. Polystyrene microplastic-induced endoplasmic reticulum stress contributes to growth plate endochondral ossification disorder in young rat. *Environ. Toxicol.* **2024**, *39*, 3314–3329. [CrossRef] [PubMed]

24. Sanjaya, S.S.; Karunarathne, W.A.H.M.; Park, S.R.; Hur, S.P.; Choi, Y.H.; Ryu, H.W.; Kim, G.Y. Tagetes erecta L. polyphenols restore osteogenesis impaired by polystyrene microplastics via NRF2-mediated ER–mitochondrial homeostasis. *Int. Immunopharmacol.* **2026**, *186*, 117055. [CrossRef] [PubMed]
25. Zhang, Y.; Cai, Z.; Luo, X.; Chen, H.; Zhang, X.; Pan, C. Exposure to polylactic acid microplastics during puberty increases the risk of skeletal dysplasia by disrupting arachidonic acid metabolism in osteoblasts. *Part. Fibre Toxicol.* **2026**, *23*, 26. [CrossRef] [PubMed]
26. Im, G.B.; Kim, Y.G.; Jo, I.S.; Yoo, T.Y.; Kim, S.W.; Park, H.S.; Hyeon, T.; Yi, G.R.; Bhang, S.H. Effect of polystyrene nanoplastics and their degraded forms on stem cell fate. *J. Hazard. Mater.* **2022**, *430*, 128411. [CrossRef] [PubMed]
27. Matovic, V.; Ljujic, B.; Miletic Kovacevic, M.; Milosevic-Djordjevic, O.; Milivojevic, N.; Nikolic, S.; Jankovic, M.G. NO-mediated DNA damage induced by polystyrene nanoparticles triggers program cell death in mesenchymal stem cells. *Drug Chem. Toxicol.* **2025**, *48*, 720–728. [CrossRef] [PubMed]
28. Najahi, H.; Alessio, N.; Squillaro, T.; Conti, G.O.; Ferrante, M.; Di Bernardo, G.; Galderisi, U.; Messaoudi, I.; Minucci, S.; Banni, M. Environmental microplastics (EMPs) exposure alter the differentiation potential of mesenchymal stromal cells. *Environ. Res.* **2022**, *214*, 114088. [CrossRef] [PubMed]
29. Kavinda, M.H.D.; Karunarathne, W.A.H.M.; Lee, K.T.; Kim, H.M.; Yang, Y.; Bae, J.Y.; Jin, C.Y.; Lee, C.S.; Choi, Y.H.; Kim, G.Y. Anthocyanin-rich polyphenols from Hibiscus syriacus activate autophagy to reverse polystyrene microplastic-induced osteogenic dysfunction. *Phytomedicine* **2026**, *150*, 157700. [CrossRef] [PubMed]
30. Liu, W.; Yang, M.; Wen, X.; Long, S.; Hu, H.; Pan, Y.; Zou, T.; Zhan, C.; Yang, F. Lipophagy suppression: A novel mechanism for developmental disruption by nanoplastics/MC-LR in zebrafish. *Environ. Int.* **2026**, *207*, 110004. [CrossRef] [PubMed]
31. Long, S.; Wen, X.; Dai, M.; Pan, Y.; Liu, W.; Zhan, C. Aged nanoplastics reprogram the ER stress-autophagy crosstalk: A mechanistic gateway to skeletal malformations in zebrafish. *Aquat. Toxicol.* **2025**, *287*, 107542. [CrossRef] [PubMed]
32. Wang, X.; Guo, S.; Li, X.; Zhao, X.; Hu, S.; Liu, R. From Carriers to Mitigators: Environmental Aging Unexpectedly Transforms Nanoplastics into Limiters of Cadmium Bioavailability in Osteoblasts. *Environ. Sci. Technol.* **2026**, *60*, 2988–3001. [CrossRef] [PubMed]
33. Pan, J.; Wang, X.; Gao, Y.; Cheng, D.; Ma, J.; Zhang, Z.; Wang, Z. Polystyrene microplastics drive chondrotoxicity in osteoarthritis through inducing ER stress and apoptosis via NFKB1 activation. *Food Chem. Toxicol.* **2026**, *215*, 116166. [CrossRef] [PubMed]
34. Di, J.; Wang, S.; Liu, L.; Rong, K.; Guo, Z.; Qin, Y.; Wang, F.; Xiang, C. Unveiling the pathogenic mechanisms of polyethylene terephthalate-microplastic-driven osteoarthritis and rheumatoid arthritis: PTGS2 signaling hub-oriented toxicity profiling. *Ecotoxicol. Environ. Saf.* **2025**, *303*, 118816. [CrossRef] [PubMed]
35. Kaur, M.; Sharma, A.; Sharma, K.; John, P.; Bhatnagar, P. Teratological, neurochemical and histomorphic changes in the limbic areas of F1 mice progeny due to co-parental polystyrene nanoplastic exposure. *Toxicology* **2025**, *511*, 154043. [CrossRef] [PubMed]
36. Yoo, S.; Moon, H.N.; Namgung, J.; Yeo, I.K. Effects of nanoplastics and 17α-ethinylestradiol exposure on skeletal development in zebrafish (*Danio rerio*) larvae. *Aquat. Toxicol.* **2026**, *297*, 107870. [CrossRef] [PubMed]
37. Zhang, X.; Xia, M.; Su, X.; Yuan, P.; Li, X.; Zhou, C.; Wan, Z.; Zou, W. Photolytic degradation elevated the toxicity of polylactic acid microplastics to developing zebrafish by triggering mitochondrial dysfunction and apoptosis. *J. Hazard. Mater.* **2021**, *413*, 125321. [CrossRef] [PubMed]
38. Liu, W.; Zeng, M.; Li, Y.; Chen, G.; Wang, J. Polystyrene nanoplastics mediate skeletal toxicity through oxidative stress and the BMP pathway in zebrafish (*Danio rerio*). *Ecotoxicol. Environ. Saf.* **2024**, *285*, 117096. [CrossRef] [PubMed]
39. Liao, J.; Qin, Y.; Yuan, Y.; Xu, S.; Zhang, R.; Liu, C. Polystyrene microplastics impair skeletal development in zebrafish: Biphasic toxicity and comparison with marine medaka. *Mar. Pollut. Bull.* **2026**, *233*, 120219. [CrossRef] [PubMed]
40. Liu, C.; Yuan, Y.; Liao, J.; Wang, Z. Polystyrene microplastics disrupt skeletal development in marine medaka Oryzias melastigma. *Environ. Pollut.* **2026**, *390*, 127498. [CrossRef] [PubMed]
41. Wang, Q.; Li, Y.; Chen, Y.; Tian, L.; Gao, D.; Liao, H.; Kong, C.; Chen, X.; Junaid, M.; Wang, J. Toxic effects of polystyrene nanoplastics and polybrominated diphenyl ethers to zebrafish (*Danio rerio*). *Fish Shellfish Immunol.* **2022**, *126*, 21–33. [CrossRef] [PubMed]
42. Li, Y.E.; Xia, Y.; Feng, L.; Chen, X.; Dang, J.; Xu, H.; Liu, Y. Combined exposure to microplastics and tetracycline leads to impaired skeletal development in young mice by the microbiota–gut–bone axis. *Ecotoxicol. Environ. Saf.* **2025**, *306*, 119308. [CrossRef] [PubMed]
43. Gao, X.; Zhang, Y.; Hou, L.; Zhao, Y.; Zhang, H.; Jia, Z.; Wang, S.; Li, H.; Pan, X.; Liu, X.; et al. Co-exposure to nanoplastics and acetaminophen causes skeletal dysplasia and behavioral abnormalities in zebrafish. *Ecotoxicol. Environ. Saf.* **2023**, *253*, 114640. [CrossRef] [PubMed]
44. Gao, Y.; Shen, W.; Xu, Z.; Zhang, Y.; Zhao, X.; Zhang, H.; Gao, X.; Jia, Z. Toxicity and transcriptome sequencing analyses of nanoplastics combined with acetaminophen on zebrafish bone development. *Ecotoxicol. Environ. Saf.* **2025**, *306*, 119363. [CrossRef] [PubMed]

45. Tarasco, M.; Gavaia, P.J.; Bensimon-Brito, A.; Cordelières, F.P.; Santos, T.; Martins, G.; de Castro, D.T.; Silva, N.; Cabrita, E.; Bebianno, M.J.; et al. Effects of pristine or contaminated polyethylene microplastics on zebrafish development. *Chemosphere* **2022**, *303*, 135198. [CrossRef] [PubMed]
46. Kessabi, K.; Abbassi, A.; Lahmar, S.; Casado, M.; Banni, M.; Piña, B.; Messaoudi, I. Combined toxic effects of cadmium and environmental microplastics in Aphanius fasciatus (Pisces, Cyprinodontidae). *Mar. Environ. Res.* **2023**, *189*, 106071. [CrossRef] [PubMed]
47. Wijaya, N.A.; Sincihu, Y.; Handoyo, H.R.; Warindra, T.; Wattimena, I. The Effect of Oral Polyethylene Microplastic Doses on Femoral Bone Cell Profiles in Wistar Rats. *Environ. Pollut. J.* **2026**, *6*, 159–169. [CrossRef]
48. Yao, M.; Guo, H.; Fang, Y.; Chen, Y.; Liu, Y.; Liu, S.; Guo, J.; Guo, Z.; Qian, J.; Ma, Q. Microplastics released from dental materials induce oral inflammatory bone resorption and apoptosis via mitochondrial dysfunction. *Environ. Int.* **2026**, *210*, 110226. [CrossRef] [PubMed]
49. Lihua, C.; Zhiyin, T. Microplastics aggravates rheumatoid arthritis by affecting the proliferation/migration/inflammation of fibroblast-like synovial cells by regulating mitochondrial homeostasis. *Int. Immunopharmacol.* **2023**, *120*, 110268. [CrossRef] [PubMed]
50. Chen, C.; Yang, Q.; Wang, W.; Lu, S.; Han, M.; He, M.; Yang, R.; Shao, W.; Zhang, C.; Song, W.; et al. Inflammatory Microenvironment Reshapes the Protein Corona of Polystyrene Nanoplastics to Exacerbate Periodontitis Progression. *Adv. Healthc. Mater.* **2026**, *15*, e71098. [CrossRef] [PubMed]
51. Gao, Q.; Rhee, C.; Maruyama, M.; Li, Z.; Shen, H.; Zhang, N.; Utsunomiya, T.; Huang, E.E.; Yao, Z.; Bunnell, B.A.; et al. The Effects of Macrophage Phenotype on Osteogenic Differentiation of MSCs in the Presence of Polyethylene Particles. *Biomedicines* **2021**, *9*, 499. [CrossRef] [PubMed]
52. Busch, M.; Bredeck, G.; Waag, F.; Rahimi, K.; Ramachandran, H.; Bessel, T.; Barcikowski, S.; Herrmann, A.; Rossi, A.; Schins, R.P.F. Assessing the NLRP3 Inflammasome Activating Potential of a Large Panel of Micro- and Nanoplastics in THP-1 Cells. *Biomolecules* **2022**, *12*, 1095. [CrossRef] [PubMed]
53. Zhang, W.; Liu, K.; Zhou, B.; Feng, D.; Li, Z.; Dai, Z.; Huang, S.; Liang, J.; Chen, S.; Wang, Z.; et al. RANKL/OPG axis as a therapeutic target for microplastic-induced bone loss: Mechanistic insights from transcriptomic and functional validation. *Toxicol. Lett.* **2026**, *415*, 111789. [CrossRef] [PubMed]
54. Dan, K.B.; Kim, K.U.; Min, H. Polystyrene Nanoplastics Disrupt Immune Cell Development and Suppress T Cell Activation via mTOR and ERK Signaling. *Biomol. Ther.* **2026**, *34*, 1255–1266. [CrossRef] [PubMed]
55. Xiong, S.; Zhao, H.; Sun, Q.; Li, X.; Qiu, H.; van Gestel, C.A.M.; Cao, L.; Wang, S.; Li, J.; Chen, G. Maternal exposure to polystyrene nanoplastics during gestation and lactation impaired skeletal growth in progeny mice by inhibiting neutrophil extracellular trap formation. *Ecotoxicol. Environ. Saf.* **2025**, *299*, 118355. [CrossRef] [PubMed]
56. Zeng, W.; He, S.; Zhao, Y.; Jiang, M.; Wang, W.; Yang, L.; Du, W.; Zhuang, W.; Guruge, K.S. Microplastics Exposure Aggravates Synovitis and Pyroptosis in SLE by Activating NF-κB and NRF2/KEAP1 Signaling. *Toxics* **2024**, *12*, 840. [CrossRef] [PubMed]
57. Li, Z.; Wang, L.; Huang, H.; Lu, D.; Han, T.; Zhao, J.; Du, G. Integrating network toxicology and in vitro validation to elucidate PET microplastic-induced osteoarthritis pathogenesis. *Front. Pharmacol.* **2026**, *17*, 1859004. [CrossRef] [PubMed]
58. Sun, R.; Xu, K.; Yu, L.; Pu, Y.; Xiong, F.; He, Y.; Huang, Q.; Tang, M.; Chen, M.; Yin, L.; et al. Preliminary study on impacts of polystyrene microplastics on the hematological system and gene expression in bone marrow cells of mice. *Ecotoxicol. Environ. Saf.* **2021**, *218*, 112296. [CrossRef] [PubMed]
59. Jing, J.; Zhang, L.; Han, L.; Wang, J.; Zhang, W.; Liu, Z.; Gao, A. Polystyrene micro-/nanoplastics induced hematopoietic damages via the crosstalk of gut microbiota, metabolites, and cytokines. *Environ. Int.* **2022**, *161*, 107131. [CrossRef] [PubMed]
60. Chintala, S.; Fathima, A.; Kakarla, R.; Jangili, R.K.; Ajumeera, R.; Jarapala, S.R.; Dumala, N. Acute oral dose toxicity study of micro- and nano-plastics of polystyrene in female Wistar albino rats. *Mutagenesis* 2026, *online ahead of print*. [CrossRef] [PubMed]
61. Guo, X.; Cheng, C.; Wang, L.; Li, D.; Fan, R.; Wei, X. Polystyrene nanoplastics induce haematotoxicity with cell oxeiptosis and senescence involved in C57BL/6J mice. *Environ. Toxicol.* **2023**, *38*, 2487–2498. [CrossRef] [PubMed]
62. Elsharkawy, E.; Abd El-Nasser, M.; El Hendy, A.; Rady, E. The Potential Immunotoxicity Induced by Long-Term Exposure to Polystyrene Nanoplastics in Rats. *Basic Clin. Pharmacol. Toxicol.* **2026**, *139*, e70303. [CrossRef] [PubMed]
63. Jiang, L.; Ye, Y.; Han, Y.; Wang, Q.; Lu, H.; Li, J.; Qian, W.; Zeng, X.; Zhang, Z.; Zhao, Y.; et al. Microplastics dampen the self-renewal of hematopoietic stem cells by disrupting the gut microbiota-hypoxanthine-Wnt axis. *Cell Discov.* **2024**, *10*, 35. [CrossRef] [PubMed]
64. Zhang, L.; Jing, J.; Han, L.; Liu, Z.; Wang, J.; Zhang, W.; Gao, A. Melatonin and probiotics ameliorate nanoplastics-induced hematopoietic injury by modulating the gut microbiota-metabolism. *Nano Res.* **2023**, *16*, 2885–2894. [CrossRef] [PubMed]


**Disclaimer/Publisher's Note:** The statements, opinions and data contained in all publications are solely those of the individual author(s) and contributor(s) and not of MDPI and/or the editor(s). MDPI and/or the editor(s) disclaim responsibility for any injury to people or property resulting from any ideas, methods, instructions or products referred to in the content.